

ECE 445
SENIOR DESIGN LABORATORY
FINAL REPORT

Anti-Lock Braking for Bicycles: Final Report

Team #36

ETHAN CHASTAIN
(ecc5@illinois.edu)

AIDAN RODGERS
(aidanfr2@illinois.edu)

LEON KU
(leonku2@illinois.edu)

TA: Nithin Balaji Shanthini Praveena
Purushothaman

May 1, 2024

Abstract

This paper describes the implementation of an anti-lock braking system (ABS) on a bicycle to improve the safety of riders. The integration of ABS aims to mitigate the risk of skidding during braking, significantly reducing the likelihood of accidents.

Contents

1	Introduction	1
1.1	Problem	1
1.2	Solution	1
1.3	Block Diagram	2
1.4	Overview of Block Diagram Subsystems	2
2	Design	4
2.1	Design Procedure	4
2.1.1	Power Subsystem	4
2.1.2	Sensing Subsystem	4
2.1.3	Braking Subsystem	5
2.1.4	Control Subsystem	5
2.2	Design Details	7
2.2.1	Power Subsystem	7
2.2.2	Sensing Subsystem	8
2.2.3	Braking Subsystem	10
2.2.4	Control Subsystem	10
3	Verification	13
3.1	Sensing Subsystem	13
3.2	Braking Subsystem	14
3.3	Control Subsystem	15
4	Costs	18
5	Conclusions	20
5.1	Discussion	20
5.2	Ethics	20
5.3	Further Work	21
	References	22
	Appendix A Requirements and Verification Table	23
A.1	Power Subsystem	23
A.2	Sensing Subsystem	24
A.3	Braking Subsystem	24
A.4	Control Subsystem	24

1 Introduction

1.1 Problem

Bicycles have consistently been popular modes of transportation. Their simplicity and affordability make them excellent for short distance commuting and recreation. However, this simplicity comes with the cost of a lack of safety features. While modern vehicles such as cars have seen major improvements in their safety features in recent years, bicycles have been relatively unchanging. This absence of safety features is dangerous. According to the National Safety Council, preventable deaths from bicycle accidents have risen 37% between 2012 and 2021 [1].

Bicycles are often prone to skidding in inclement weather conditions, increasing the risk of injury. While other modern vehicles have long since implemented safety features such as anti-lock braking systems (ABS) to combat the risk of brake locking, bicycles have not.

1.2 Solution

Adding safety features already implemented in modern cars to bicycles could begin to address the issue of the lack of bicycle safety features. Implementing ABS onto bicycles would greatly reduce the risk of wheels locking up under poor ambient conditions, preventing dangerous skidding from occurring and improving their safety. Adding this feature while maintaining the affordability of bicycles has potential to reduce the number of traffic collisions involving bicycles and thus reduce the number of preventable cyclist injuries and deaths. In this project, a successful prototype of an anti-lock braking system is implemented on a bicycle provided by the machine shop at the Electrical and Computer Engineering building. The ABS is able to accurately measure wheel speed, detect wheel locking, and modulate braking accordingly so that the bicycle is able to come to a stop more effectively. The ABS consists of four subsystems that interact with each other, outlined in more detail in Sections 1.3 and 1.4 – the power subsystem, sensing subsystem, braking subsystem, and control subsystem. Essentially, the power subsystem provides power to the other subsystems. The sensing subsystem detects rotations of the front and rear bicycle wheels, producing a digital signal that is sent to the control subsystem. The control subsystem detects slip, and if the user applies the brakes by pressing the brake button, the control subsystem outputs a signal to the motor driver to operate the servo motor, pulling the brake cable.

1.3 Block Diagram

The block diagram of the anti-lock braking system is shown in Figure 1.

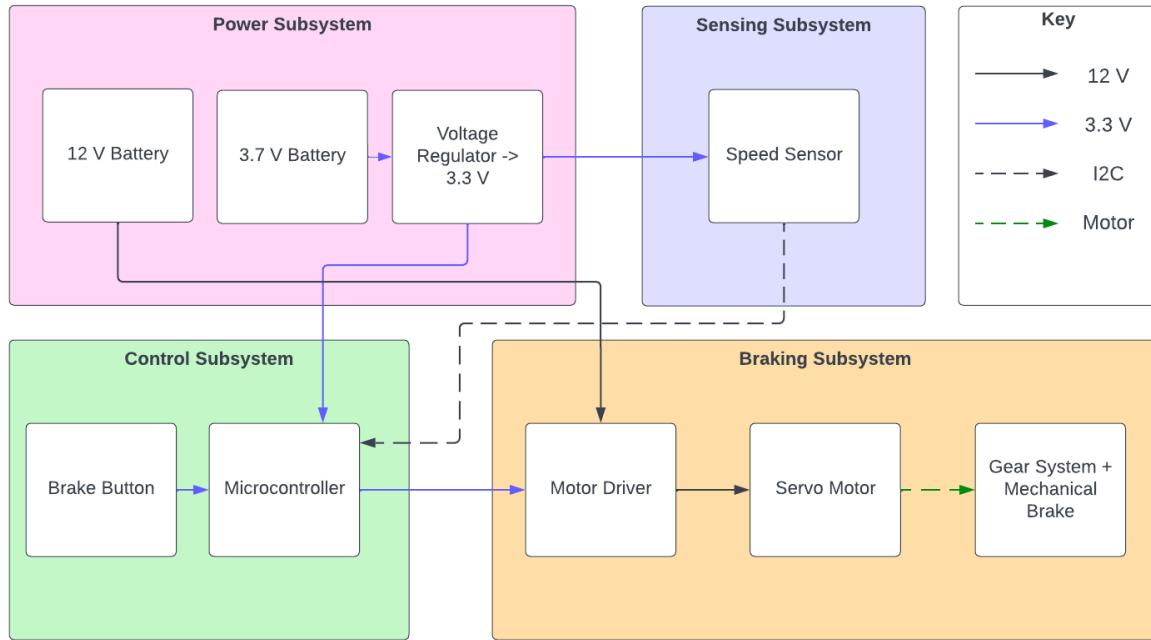


Figure 1: Block diagram of the anti-lock braking system.

1.4 Overview of Block Diagram Subsystems

To briefly describe the block diagram in Figure 1 for our project, each of the subsystems will be expounded upon. First, the power subsystem is comprised of a 12 V nickel metal hydride (NiMH) battery and a 3.7 V lithium-ion polymer (LiPo) battery. The 12 V battery is used to power the motor driver. The 3.7 V battery is regulated using a low dropout regulator to 3.3 V and is used to power to the sensors, microcontroller, and motor driver logic. Next, the sensing subsystem, when powered by the power subsystem, is able to effectively detect the individual wheel speeds of the bicycle. The sensing subsystem accomplishes this by detecting changes in magnetic flux. Following the detection of changes in magnetic flux, the sensing subsystem outputs a square wave to the control subsystem. Next, the braking subsystem receives a control input from the control subsystem that describes when to brake. The braking subsystem accomplishes braking by tensioning the cable connected to the bicycle's rear wheel brake calipers via stepper motor. Lastly, the control subsystem employs logic to determine the output to the braking subsystem based upon inputs received from the sensing subsystem. This logic includes knowing when to brake, for how long to brake, and, for debugging purposes, the theoretical forces acting upon the system. Additionally, the control subsystem is able to interpret the square waves coming from the sensors as wheel angular velocities. Then, regarding the output to the

braking subsystem, the control subsystem enables the motor driver and outputs the step resolution, the number of steps the motor should take, and the direction the motor should turn.

Next, for a description of the major changes to the block diagram from our proposal. First is a change to the power subsystem: our original design had intended to use a single 5 V battery with a battery management system and a voltage regulator to supply 5 V to the entire project. However, the motor driver that was ultimately used in the project required much higher voltages and the battery management system was determined to be unnecessary. In the final design, the power subsystem used two different batteries, one for the motor driver, and one for the remaining components. In addition, the final design included a motor driver with the braking subsystem, the necessity of which was neglected during the original design process.

As for what our project must accomplish in order for our project to be considered successful are some high-level requirements:

- This project must possess the ability to accurately determine bicycle wheel angular velocity at any point in time and consequently be able to prevent brake lock-ups.
- This project must demonstrate the advantages of Anti-Lock Braking (ABS) over traditional braking in emergency situations; this includes coming to a stop faster on adverse road conditions (shorter stopping distances) and the ability to maneuver while braking.
- This project must display the responsiveness required of ABS; the project must show that within one second of the brake system receiving input, the brakes will begin actuating from the ABS control.

2 Design

2.1 Design Procedure

2.1.1 Power Subsystem

As the project was intended to be portable, it was necessary that batteries be used to supply power to the control, sensing, and braking subsystems. The size, rated voltage, and capacity of the batteries used in the power subsystem were determined by the components of the other subsystems. Inspection of the component datasheets indicated that the microcontroller and Hall effect sensors require a supply voltage in the range of 1.7 to 3.6 V [2] [3]. The motor driver logic must operate in the range of 2 to 5.5 V, the motor driver reference input voltage must be in the range of 0 to 3.6 V, and the motor power supply must be in the range of 10 to 47 V [4].

Based on these specifications, it was apparent that two different power supplies would be necessary for this project – one for the motor power supply, and one for the remainder of the components. A 3.3 V power supply was determined to be sufficient for use with the microcontroller, Hall effect sensors, and motor driver logic and reference input. To realize this power supply, a 3.7 V (nominal) LiPo battery was chosen along with an AZ1117I 3.3 V low-dropout regulator (LDO). The LiPo battery was chosen due to its low weight and high energy density. An LDO was chosen rather than a typical linear regulator because of the fact that the input voltage would be close to the output voltage. According to its datasheet, the LDO chosen for the project can supply 3.3 V, $\pm 1\%$, for load currents up to 1.35 A [5]. Since these specifications satisfied the subsystem level requirements, the LDO was deemed suitable for use with the project.

This left only the motor power supply. According to the motor driver datasheet, the output current has a typical value of 1.5 A while active [4]. Therefore, a battery with sufficient capacity would be necessary to supply the large amount of current necessary to operate the motor. To supply power to the motor, a 10 cell, 12 V, NiMH battery (CMP-AAA-75-37) was selected, due to the lower cost and improved safety of NiMH batteries over lithium-ion batteries. The 750 mAH capacity of proved to be sufficient for supplying the necessary current to the motor.

2.1.2 Sensing Subsystem

The purpose of the sensing subsystem is to accurately determine the wheel speed. To accomplish this, the sensing subsystem employs a first-order infinite impulse response (IIR) filter. As for a decision on choices of sensors that could accomplish the goal of this subsystem, an optical encoder was initially considered for use with the sensing subsystem. However, after further research, it was ultimately decided that a Hall effect sensor should be used instead. This decision was made due to the higher costs and complexity associated with using an optical encoder compared to using a Hall effect sensor.

Originally, we selected the TMAG5273 linear Hall effect sensor as our only standard was that the sensor had to be able to operate with a supply of 3.3 V. After designing the first

iteration of the PCB, we realized that this model had glaring issues. The fact that the TMAG5273 outputs an analog signal brought about problems. With analog signals, each transition comes with rise times and fall times. If this delay time is too large, the measured wheel speed may be inaccurate. Therefore, an additional edge detection would need to be added to produce a more discrete signal. Additionally, when programming with the STM32CubeIDE, it is easier to analyze digital signals than analog signals.

Because of these reasons, we agreed to use a different Hall effect sensor, specifically, a DRV5011 digital latch Hall effect sensor. This sensor is essentially a magnetic switch that outputs a digital signal, i.e., a signal with either logical high or low values. Placing the sensor in close proximity to a magnet toggles the switch. The North pole of the magnet causes the sensor to output a high value, and the South pole of the magnet causes the sensor to output a low value.

2.1.3 Braking Subsystem

The braking subsystem revolves around the choice in motor used to pull the braking cable in the bicycle. That being the case, the pertinent choices for a motor fall between a stepper motor and a DC motor. A stepper motor has advantages in which the orientation of the motor can be identified and known from initialization. A DC motor has advantages in regards to the speed by which the motor actuates. Additionally, DC motors can generally output more torque than a stepper motor. For our braking subsystem, we decided to use a stepper motor because we value the ability to know the orientation of the motor. We also use the known states as a way to identify the minimum actuation distance needed to supply sufficient braking. In this manner, we are able to bolster the slower actuation speed concomitant with stepper motors.

As a result of our decision to use a stepper motor to drive the cable in the bicycle, a gear system is required to generate the necessary torque. As opposed to common gear reduction trains, the gear train we use involves a worm gear meshed with a relatively higher-toothed spur gear. The decision to use a worm gear was made due to the characteristic of worm gears to be non-backdrivable. In this manner, backdriven electromotive force (EMF) will not be a concern for the stepper motor.

Lastly, the actuation rate of a motor is generally related to the power supplied to the motor. In correlation with this, the choice for a stepper motor driver would need to be a driver capable of handling large supply voltages. In this manner, we will also be able to actuate the motor itself in a timely manner.

2.1.4 Control Subsystem

Regarding our choice of microcontroller for the project, there are many microcontroller units (MCUs) to choose from. The microcontroller we settled on was chosen for ease-of-use when considering the usage of an ST-Link and because the MCU came with a Floating-Point Unit (FPU). We desired a FPU because the controller we wanted to implement utilized floating-point numbers. While entirely possible to perform calculations

using floating point numbers scaled to integer values, it is undesirable in regards to the unnecessary burden this would have on the runtime of the processor. In which it would take many more clock cycles to perform floating-point operations without a FPU.

Regarding the choice of a trigger for the control subsystem to activate, there were many potential choices. Choices for a bicycle trigger could be a switch or button, and a trigger choice specifically for an ABS design could be a dial. We ended up using a button over a switch to represent the activation of the control subsystem because a button most closely resembles bicycle brake handles in terms of usage. In which a bicycle brake handle must be depressed when the brakes should be in use. A dial was considered for the trigger to our control subsystem because bicycle brake handles also serve to have differentiated braking aggressiveness in how much the handle is depressed. A dial can introduce the same differentiated braking hardness in allowing for more information to enter the control subsystem; this information can be used to change the behavior of the ABS braking. Ultimately, the decision to use a button won over a dial due to challenges involving the time to implement and the added complexity in the system. For the scope of the control subsystem in the project, the requirements for the subsystem do not require differentiated braking capabilities, and so a dial adds unnecessary challenges.

Lastly, an introduction to the critical equation emplaced in the control subsystem and the tooling used in the control subsystem.

First is the relative slip estimation equation:

$$\text{slip} = 1 - \frac{\omega_w}{\omega_v} \quad (1)$$

Finally, the tooling used in the control subsystem is MATLAB Simulink; used to generate embedded code from a discretized model of a controller.

Figure 2 below depicts a Simulink model of the lowest level design of the Anti-Lock Braking System (ABS) controller. In which it is apparent that there will necessarily be floating-point operations in the equation critical to the system.

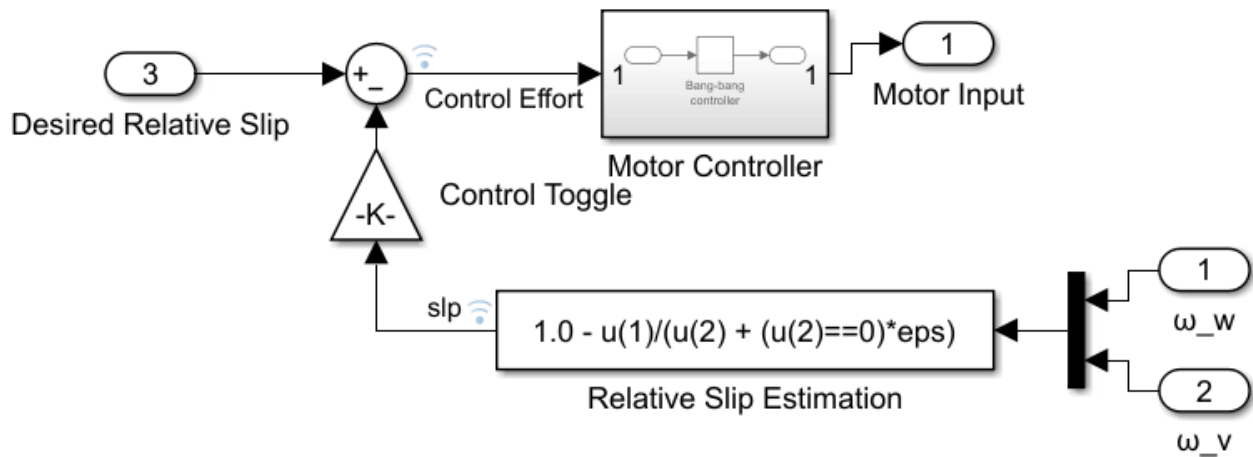


Figure 2: Minimal Design of the ABS Controller

2.2 Design Details

2.2.1 Power Subsystem

The design for the power subsystem was rather simple, mainly consisting of circuitry for use with the linear regulator. For the PCB implementation, the recommended application of the LDO was followed, which is shown in Figure 3.

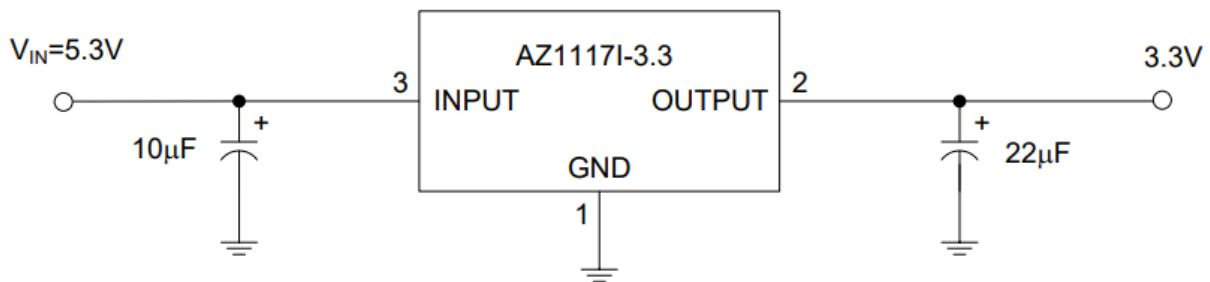


Figure 3: Recommended application circuit for the AZ1117I LDO [5].

As shown in the circuit schematic, capacitors were added in parallel with the input and output to reduce the voltage ripple and improve the stability of the LDO. The 3.7 V LiPo battery was connected to the input of the LDO. The 3.3 V output of the LDO was connected to the power supplies of the Hall-effect sensor and microcontroller. The output of the LDO was also used as the motor driver input reference voltage and as the power supply for the motor driver logic. The 12 V NiMH battery was connected directly to the motor driver power supply (V_{CC}).

2.2.2 Sensing Subsystem

As mentioned in Section 2.1.2, we decided to use the DRV5011 Hall effect latch. When the sensor is in close proximity to the positive pole of a magnet, the output produces a rising edge. When the sensor is in close proximity to the negative pole of a magnet, the output produces a falling edge. The design of the sensing subsystem involves placing magnets with alternating poles onto the wheel, so that with each rotation, the Hall effect sensor outputs several cycles of pulse-width modulated (PWM) signals. By measuring the time between each rising edge, the microcontroller will then be able to correctly determine the rotational speed of the wheel.

The integration of the magnets and the Hall effect sensor onto the bicycle is shown in Figure 4.



Figure 4: Placement of the magnets and Hall effect sensor on the bicycle wheel.

As shown in Figure 4, the Hall effect sensor is placed close enough to the magnets such that it can accurately detect the changing magnetic field. With four magnets, the sensor outputs two rising edges and two falling edges with each rotation. The signal is then sent to the microcontroller and picked up using the interrupt function, where we can choose to pick up rising edges, falling edges, or both. By using the HAL_GPIO_EXTI.Callback function, as shown in Figure 5, the microcontroller is able to capture each wheel rotation correctly.

```
void HAL_GPIO_EXTI_Callback(uint16_t GPIO_Pin) {
// HAL_GPIO_WritePin(GPIOA, GPIO_PIN_5, GPIO_PIN_SET);
  if (GPIO_Pin == GPIO_PIN_13){
    mode = mode + 1;
    count++;
  }
  if (mode > 3)
    mode = 0;

  if (GPIO_Pin == GPIO_PIN_4){
//    delta(&delta_t1,&t1);
//    wheel_speed = IIR(rad/delta_t1,wheel_speed);
//    wheel_speed = 30/delta_t1;

    float tmp = HAL_GetTick();
    delta_t1 = tmp - t1;
    t1 = tmp;
//    wheel_speed = 30/delta_t1;
    wheel_speed = IIR(rad/delta_t1,wheel_speed);
    count2++;
  }
}
```

Figure 5: Example of using the HAL_GPIO_EXTI.Callback function.

One important decision that arose when designing the sensing subsystem regarded the question of how many magnets should be placed onto the bike. By having more magnets, the Hall effect sensor outputs more rising edges per rotation. Since wheel speed is calculated by measuring the time between rising edges, having more magnets meant that the microcontroller could update the wheel speed more accurately.

There were other factors to take into consideration. It is reasonable for a bicycle to have speeds from 20-25 km/hr. If the bike wheel has a 2 m circumference, the wheel would turn two times per second. With four magnets bringing two rising edges per rotation, the microcontroller would have to correctly capture four rising edges within a second. With eight magnets, the microcontroller would have to capture eight rising edges per second.

Unfortunately, the interrupt function is not fast enough to accurately capture all eight rising edges. By modeling the signal with a waveform generator, starting with six magnets, the measured wheel speed starts to fluctuate. At eight magnets, the measured wheel speed becomes very unstable. Therefore, the final design used four magnets to maximize the PWM signal frequency while keeping a reliable estimate of wheel speed.

2.2.3 Braking Subsystem

For the gear train in the braking subsystem, while the gears were provided and so have unknown tooth pitch, the spur gear is estimated to be 90 tooth and the worm gear appears to be single start. Assuming the gear pitch is a reasonable estimate, the gear ratio for the gear train can be estimated to be 90:1. In this case, the driven torque by the motor is estimated to be 90 times higher.

Regarding the brake force applied to the rear wheel of our system, while not explicitly measured, it was found that 5000 steps of the stepper applies full braking. By full braking, it is meant that the rear wheel can no longer spin. Additionally, it is known that the step angle of the stepper motor is 1.8 degrees, so this translates to 25 complete turns of the stepper motor by Equation 2.

$$5000 \text{ steps} \cdot \frac{1.8^\circ/\text{step}}{360^\circ/\text{turn}} = 25 \text{ turns} \quad (2)$$

2.2.4 Control Subsystem

To introduce the finer details of the control subsystem, two separate models for the controller will need to be introduced.

First is the practical controller model, shown in Figure 6.

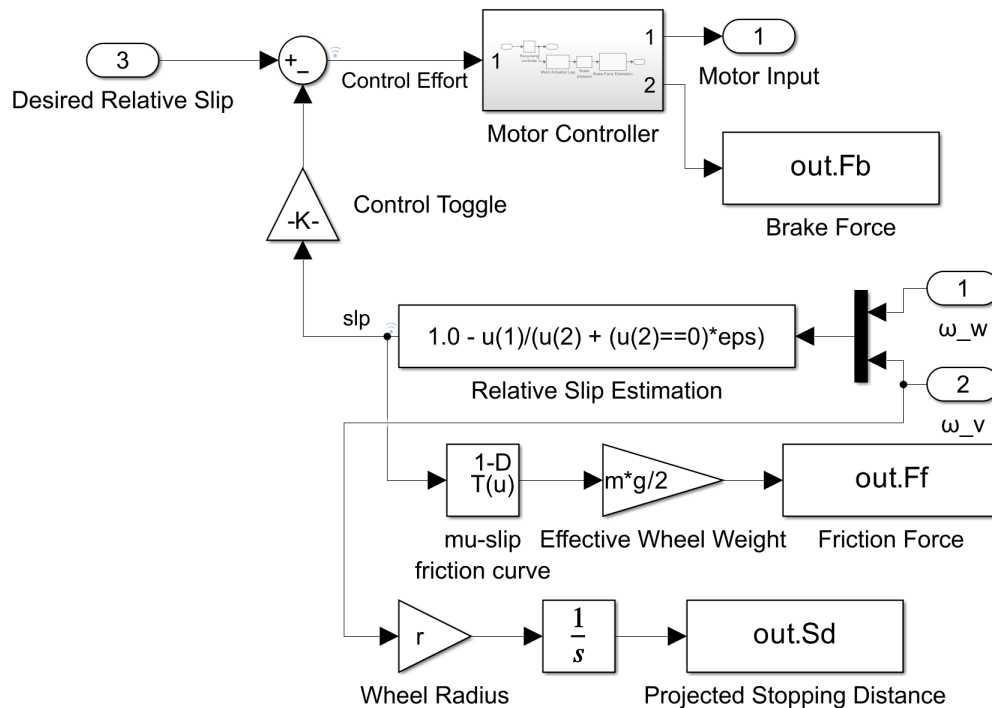


Figure 6: Practical Implementation Design of the ABS Controller

Next is the simulation controller model, shown in Figure 7.

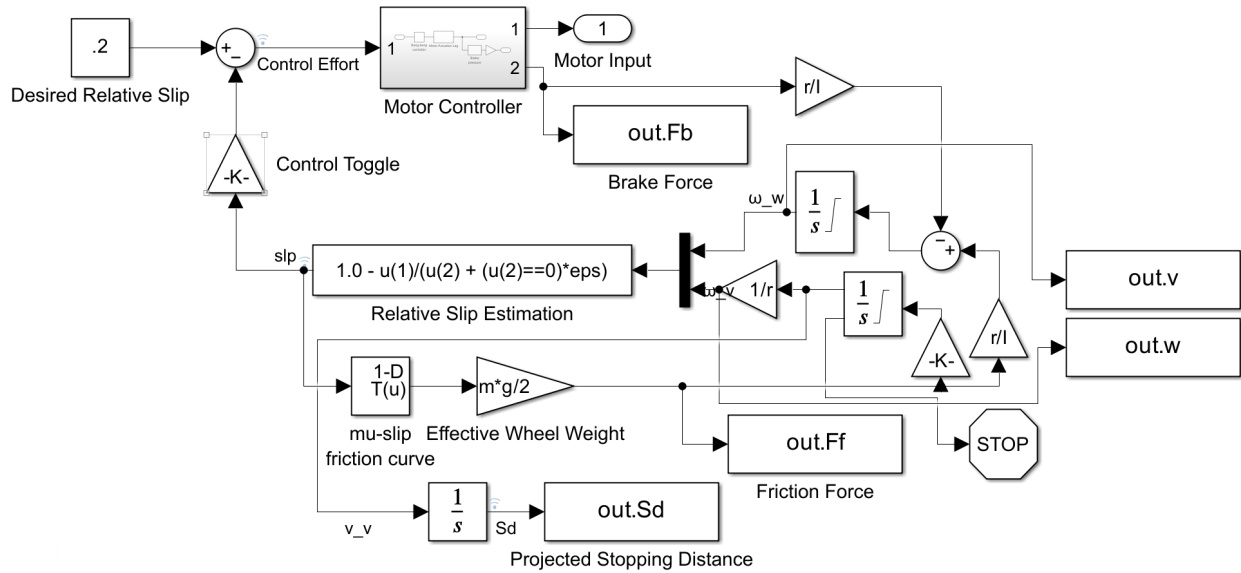


Figure 7: Design of the ABS Controller for Simulation

The critical equation is used in both models because anti-lock braking systems operate on the principal of slip.

Regarding the differences between the practical controller design and the controller design geared towards simulation, the simulation design must contain a proper model of the mechanics behind a braking bicycle. Unlike in a practical environment where the bicycle mechanics can be sampled via sensors, when simulating, the bicycle mechanics must be theoretically accurate and solvable.

Different in both controllers from the minimal design of Figure 2 are the inclusion of the force of braking, the force of friction, and the projected stopping distance as outputs. These outputs are added to gain additional insight into the efficacy of the controller—and the system as a whole—through data.

In order for the controllers to output meaningful data, the physical constants of the bicycle required identification or accurate estimation. The following table, Table 1, relates the constants in the controller models to their actual or reasonable values.

g	$9.81 \frac{m}{s^2}$
r	$0.33 m$
I	$0.392 kg \cdot m^2$
m	$9.525 kg$

Table 1: Bicycle Physical Constants

Additionally, within the embedded code flashed onto the microcontroller were some additions to the logic established in the Simulink model. These additions simply assert complete braking if the wheels are determined to not be spinning or assert no braking if the brake trigger has not been depressed.

3 Verification

3.1 Sensing Subsystem

To demonstrate that the sensing subsystem accurately determines the wheel speed, a variable, *count*, has been implemented that increments every time a rising edge is received from the Hall effect sensor. The value of *count* is plotted against time in Figure 8.

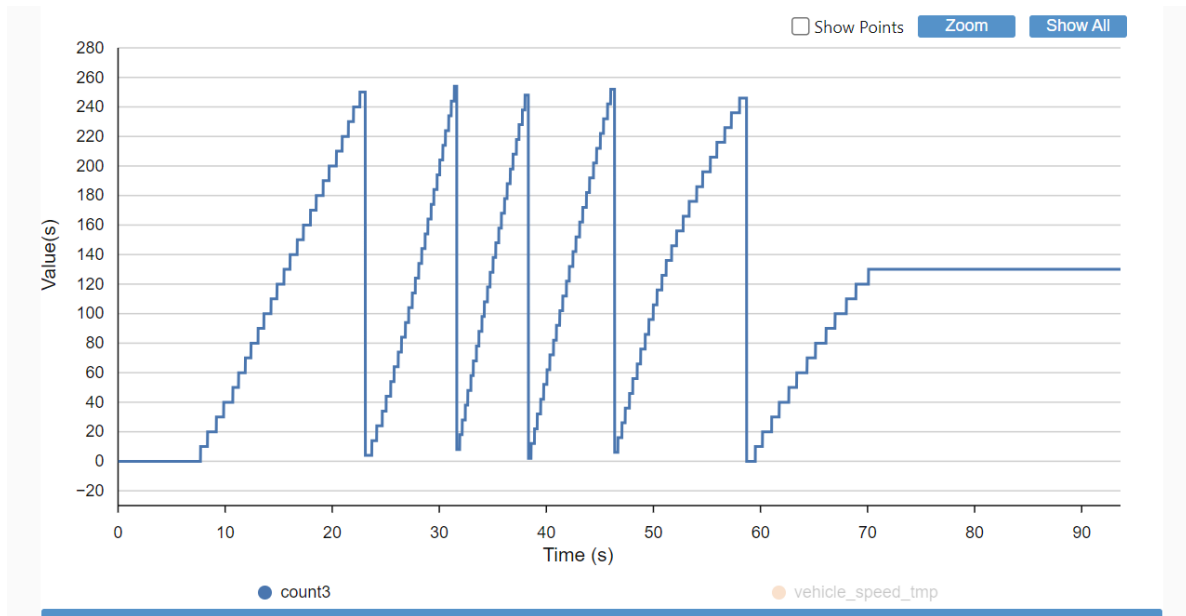


Figure 8: Graph of *count*, incrementing every rising edge, against time.

The corresponding wheel speed is plotted against time in Figure 9.

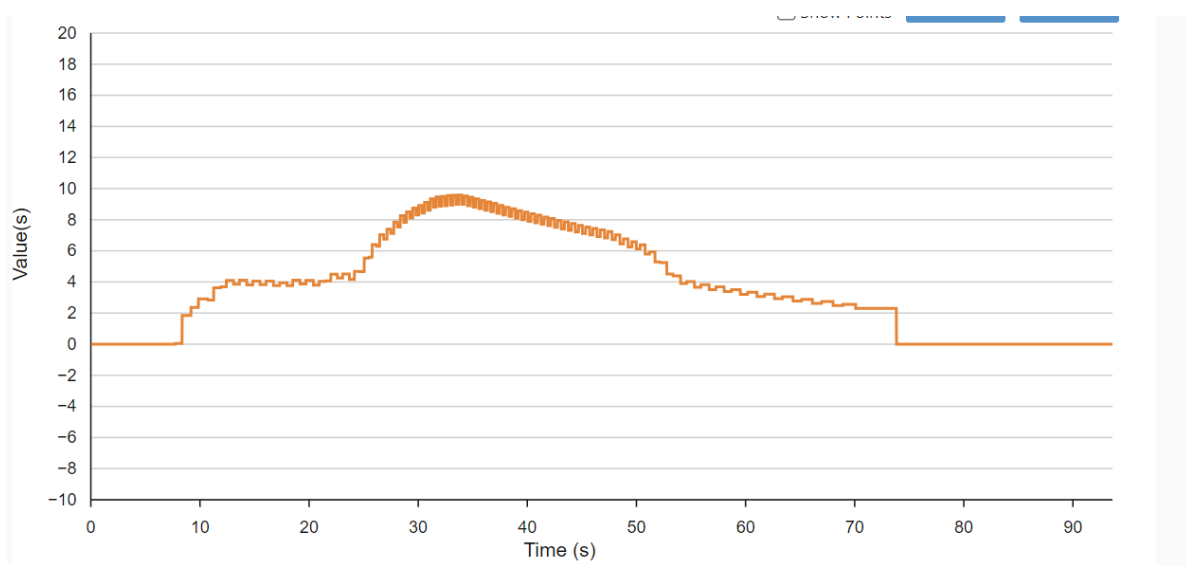


Figure 9: Graph of wheel rotational speed against time.

Analyzing the graph of *count* in Figure 8, between 10 and 20 seconds, *count* is slowly incrementing. Between 25 and 40 seconds, *count* is incrementing at a faster rate. This indicates that the time between rising edges is shorter between 25 and 40 seconds. After 45 seconds, the rate at which *count* increments drops again.

Now, analyzing the graph of wheel speed in Figure 9, it is clear that between 25 and 40 seconds, the speed is the highest. After 45 seconds, the wheel speed continuously decreases.

Therefore, it is clear that the sensing subsystem is accurately detecting each wheel rotation and, more importantly, calculating the wheel speed correctly.

3.2 Braking Subsystem

To verify the braking subsystem, it was first necessary to find the RPM of the stepper motor in our configuration. An empirical measurement of the RPM yielded 108 RPM. This measurement was acquired by measuring the period it took the motor to complete a certain number of revolutions. The average time period per revolution was found to be 0.56 seconds. Thus, 108 RPM, which satisfies our requirement for the RPM of the motor to be greater than 100 RPM.

Using a torque-speed curve from a retailer, shown in Figure 10, the amount of torque driving the cable can be estimated [6].

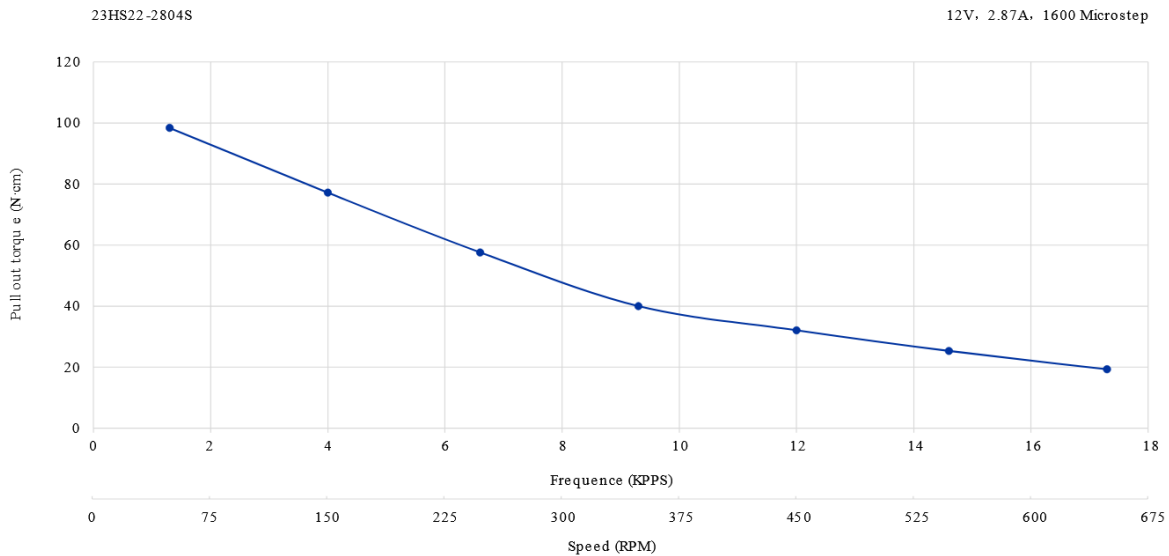


Figure 10: Plot of torque versus RPM.

From the plot, it can be found that the torque delivered to the shaft of the motor can be expected to be close to .87 N-m. So, the torque experienced by the cable pulling the brake is expected to be 78.3 N-m.

In our project, the brake calipers were successfully engaged by the braking subsystem,

so the braking subsystem satisfies the requirement for actuation of the bicycle brakes. In which case 78.3 N-m is sufficient to actuate the brakes of the bicycle.

3.3 Control Subsystem

For the verification of the control subsystem, we needed to verify that our signal achieves better step response characteristics than the characteristics provided in A.4.

Our controller choice, bang-bang, is an optimal controller type that necessarily meets step response characteristics by virtue of being an optimal controller. However, this must be verified.

To begin this verification process, it was necessary to check simulations of the controller output and also the actual output of the controller when embedded on a MCU. The below figures (11 & 12) represent the simulation output to test signals and the actual output with real signals.

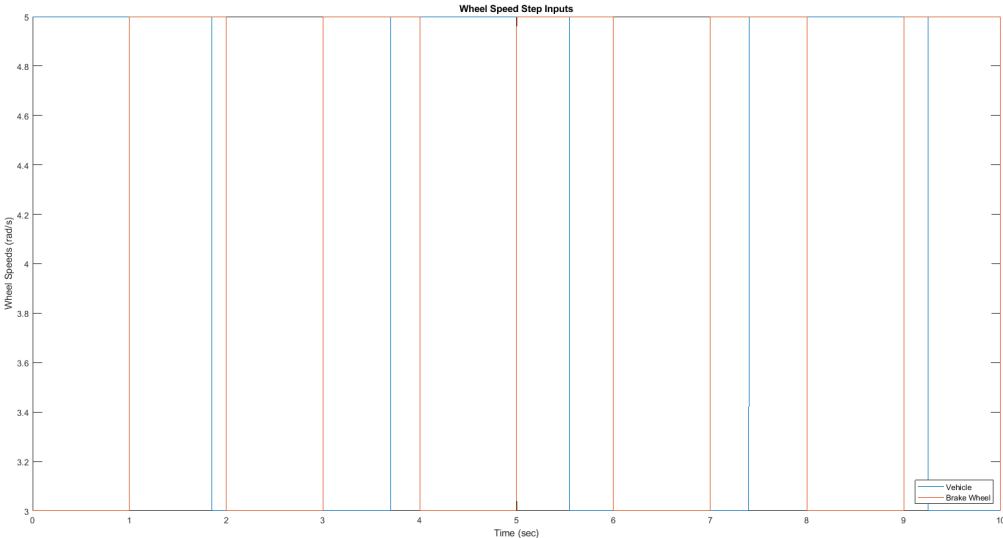


Figure 11: Step Input Test Signals

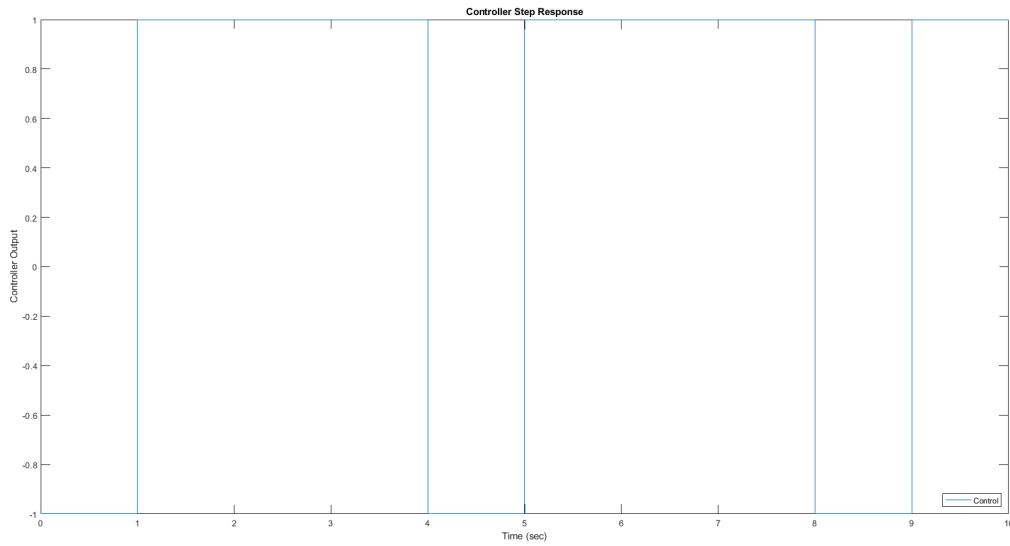


Figure 12: Controller Response to Step Input Test Signals

From the plot of the controller response, we can see that the controller already meets the specifications. That is, the controller currently performs better than the specifications tabularized in Appendix A.

However, simply simulating the controller is not necessarily indicative of the controller performing the same in real-time. That is why the controller must also be tested in a real environment.

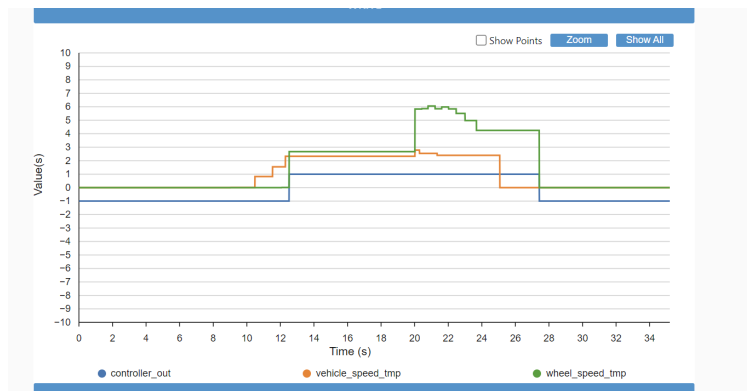


Figure 13: Controller Response to Step Input Test Signals

To interpret the data within Figure 13, we must identify the conditions under which the controller should output high and when the controller should output low. When the rear wheel (*wheel_speed* variable) is spinning faster than the front wheel (*vehicle_speed* variable), we expect the controller to output high.

We can see in Figure 13 that the controller output does indeed immediately toggle to its high output as soon as the rear wheel begins spinning faster than the front wheel. Next, we can see that the output also returns to low as soon as the rear wheel speed is determined to be zero. This behavior is exactly what we want our control subsystem to be exhibiting, and therefore the control subsystem meets all of its requirements.

4 Costs

The components used in this project and their costs are tabulated in Table 2.

Description	Manufacturer	Part	Quantity	Cost
Low-Voltage, Digital-Latch Hall Effect Sensor	Texas Instruments	DRV5011	2	\$0.94
Arm Cortex-M4 32-bit MCU+FPU	ST Microelectronics	STM32F401-RCT6TR	1	\$6.49
CLOCK-in controlled Bipolar Stepping Motor Driver	Toshiba	TB67S109AFNG	1	\$3.61
Low Dropout Linear Regulator with Industrial Temperature Range	Diodes Inc.	AZ1117I	1	\$0.38
Crystals 12MHz 20pF	Vishay	73-XT49S1200-20	5	\$2.80
Nema 23 Stepper Motor Bipolar	Oyostepper	23HS22-2804S	1	\$19.87
Stepper Motor Driver Compact Carrier	Pololu Corporation	TB67S249FTG	1	\$12.95
Stepper Motor Driver Compact Carrier - Full Breakout	Pololu Corporation	TB67S249FTG	1	\$14.95
CONN RCPT 6POS 0.1 GOLD PCB R/A	Samtec Inc.	SSW-106-02-F-S-RA-ND	3	\$2.85
CONN HEADER VERT 10POS 2.54MM	Würth Elektronik	732-2672-ND	3	\$1.29
BATTERY PACK NIMH 12V AAA	Dantona Industries	CMP-AAA-75-24	1	\$29.95

NUCLEO-64 STM32F401RE EVAL BRD	ST Microelectron- ics	497-14360-ND	1	Borrowed
PCB Assembly and Shipping	PCBWay	-	20	\$40.40
SMD Resistors and Capacitors	-	-	-	Free
Bicycle	-	-	1	Free
Total				\$136.48

Table 2: List of project components and their costs.

According to this analysis, the total cost of the components used in this project is \$136.48. Labor costs must also be taken into account. Assuming a salary consistent with the average starting salary of electrical engineering graduates at the university of Illinois, \$88,321, a reasonable estimate of an hourly wage would be \$44/hour for a 40 hour work week [7]. Estimating that each member spent 10 hours a week over the 16 week semester, the total labor costs are estimated to be

$$\text{Labor cost} = (\$44/\text{hour})(10 \text{ hours}/\text{week}/\text{person})(16 \text{ weeks})(3 \text{ people}) = \$21,120 \quad (3)$$

This brings the total estimated cost of the project to be

$$\text{Total cost} = \text{Component cost} + \text{Labor cost} = \$136.48 + \$21,120 = \$21,256.48 \quad (4)$$

5 Conclusions

5.1 Discussion

While developing this project, the group ran into challenges. This project was the group's first time implementing a control system on a microcontroller and designing a control system outside of a structured, class setting. Poor communication during certain weeks prevented the group from effectively working together. Poor communication also prevented the group from successfully implementing the design onto a PCB, due to a misunderstanding regarding the specific microcontroller model used in the project. Additionally, the bicycle dynamics were originally represented very poorly, so the controller design aspect was delayed by the time it took to generate proper figures using a theoretical controller design.

Despite these challenges, throughout the course of the semester, we were able to successfully design, build, and test a prototype anti-lock braking system on a bicycle. The ABS is able to measure wheel speed, detect brake slipping, and modulate braking accordingly with quick actuation responsiveness, demonstrating the advantage of anti-lock braking systems over traditional braking and satisfying all of the high-level requirements set in our revised design document.

This project potentially has implications for the future of bicycle safety. A commercially successful integration of an ABS onto a bicycle could lead to a reduction in cyclist injuries and fatalities. It could also start a trend of implementation of other safety features onto bicycles, such as traction control, brake assist, and automatic emergency braking. As electric bicycles rise in popularity, similar ABS systems could likely also be more easily integrated with them as well.

5.2 Ethics

As improving the safety of bicycles was the motivation behind this project, the group was sure to closely follow ethical standards while designing and building the ABS.

The IEEE Code of Ethics stresses the importance of solving technical problems only when one is trained with proper experience [8]. This group consists of electrical engineers with little background in mechanical engineering, which makes it crucial to seek advice from other experts in the mechanical engineering field. Indeed, the group has been regularly communicating with the machine shop as well as professors in mechanical engineering about the project.

The IEEE Code of Ethics also states that it is important "to hold paramount the safety, health, and welfare of the public" [8]. While the group worked hard to ensure the safety of this project, there are still ethical issues to consider. The braking subsystem uses a motor to mechanically engage the brakes. The motor rotates a gear system that pulls on a brake cable. Given that brakes naturally wear down over time, a system to monitor their condition might be necessary to alert the user of potential issues. Therefore, it is important to test the ABS with well conditioned brakes.

Accidentally or intentionally, a malfunctioning ABS can lead to serious injuries due to the significant increase in stopping distance. Therefore, another possible improvement to improve the project's compliance with the IEEE Code of Ethics would be to have a indicator showing whether our ABS is malfunctioning or in danger of malfunctioning, whether the cause is due to low battery or something else.

5.3 Further Work

While the project was ultimately successful, there is still much room for improvement upon the design and implementation. Most importantly, the group was unsuccessful in implementing the circuitry onto a PCB. Further work would certainly involve the successful integration of the subsystems onto an enclosed PCB. One major flaw in the design involved the mechanical gear ratio of the braking subsystem. The gear train was left over from a previous project and thus was not designed with this project in mind. This resulted in the braking speeds being significantly slower than desired. A future redesign of the project would involve changing the gear ratio to improve the mechanical braking response. Other potential improvements relate to user experience and aesthetics, such as acquiring a bike seat, limiting the amount of wires, and overall improving the outside appearance of the design.

References

- [1] N. S. Council. ""Bicycle Deaths"." (2024), [Online]. Available: <https://injuryfacts.nsc.org/home-and-community/safety-topics/bicycle-deaths/> (visited on 05/01/2024).
- [2] *Arm Cortex-M4 32-bit MCU+FPU, STM32F401xC*, Rev. 11, STMicroelectronics, Apr. 2019.
- [3] *Low-Voltage, Digital-Latch Hall Effect Sensor, DRV5011*, Rev. B, Texas Instruments, Jan. 2020.
- [4] *CLOCK-in controlled Bipolar Stepping Motor Driver, TB67S109AFTG/FNG*, Toshiba, Feb. 2020.
- [5] *Low Dropout Linear Regulator with Industrial Temperature Range, AZ1117I*, Rev. 2-2, Diodes Incorporated, Sep. 2022.
- [6] StepperOnline. ""Nema 23 Bipolar 1.8deg ..."" (2024), [Online]. Available: <https://www.omc-stepperonline.com/nema-23-bipolar-1-8deg-1-26nm-178-4oz-in-2-8a-2-5v-57x57x56mm-4-wires-23hs22-2804s> (visited on 05/01/2024).
- [7] G. C. o. E. University of Illinois. ""Electrical Engineering"." (2024), [Online]. Available: <https://grainger.illinois.edu/academics/undergraduate/majors-and-minors/electrical-engineering> (visited on 05/01/2024).
- [8] IEEE. ""IEEE Code of Ethics"." (2016), [Online]. Available: <https://www.ieee.org/about/corporate/governance/p7-8.html> (visited on 02/08/2020).

Appendix A Requirements and Verification Table

A.1 Power Subsystem

Requirements	Verification
The power subsystem must be able to supply up to 100 mA at 3.3 V with 2% peak-to-peak voltage ripple.	To verify the voltage and current output of the power subsystem, a digital multimeter (DMM) and an electronic load will be used. The input of the system will be connected to the battery. The output of the system will be connected to the DMM and electronic load, which will measure the voltage and current output, initially under no load conditions. The electronic load will then be set to 100 mA, and the voltage will be measured again with the DMM. For both conditions, the voltage must be within the range of 4.9 to 5.1 V.
The power subsystem must operate at an efficiency greater than 90% for loads of up to 100 mA.	To verify the efficiency of the power subsystem, two wattmeters will be used. The input of the voltage regulator will be connected to one wattmeter, and the output of the voltage regulator will be connected to the other. The output power will be measured with the other wattmeter. The efficiency, defined as the output power over the input power, will be calculated for loads of up to 100 mA. The efficiency must be 90% or greater for all loads.

A.2 Sensing Subsystem

Requirements	Verification
The Hall effect sensors must accurately indicate each wheel turn.	Spin the wheels and compare the observed speed with the recorded speed.
The sensor must create a steep spike to indicate each spin.	Observation of the digital output signal of the Hall effect sensor.

A.3 Braking Subsystem

Requirements	Verification
The driver has to drive the motor at least 100 RPM in order to perform a quick stop.	Measure rotational speed using the Hall effect sensor.
The motor and gear system must provide enough force to pull the brake cable.	Measure the distance between the brake caliper and the rim (they should be touching), and see if a successful brake is performed.

A.4 Control Subsystem

Requirements	Verification
Motor Controller Rise Time $t_r \leq 75$ ms	Simulation of the Motor Controller's step response and by plotting data collected from the system.
Motor Controller Settling Time $t_s \leq 120$ ms	Simulation of the Motor Controller's step response and by plotting data collected from the system.
Motor Controller Maximal Peak Ratio $M_p \leq 15\%$	Simulation of the Motor Controller's step response and by plotting data collected from the system.